Resonant-Inductive Degeneration for Manifold Improvement of Phase Noise in Bipolar LC-Oscillators

Aleksandar Tasić, Wouter A. Serdijn, and John R. Long

***Abstract*—Resonant-inductive degeneration of bias current source is described in this paper as a method for a manifold improvement of phase noise in inductance–capacitance (*LC*) voltage-controlled oscillators. For the verification of this phase-noise reduction method, a test bipolar *LC*-oscillator has been designed using a phase-noise model obtained from the spectral noise analysis. By forming a resonance at twice the oscillation frequency in the emitter of the bias current source transistor, phase noise of the *LC*-oscillator is improved by 6 dB. Phase noise of −112 dBc/Hz at 1 MHz offset from a 5.7 GHz-band carrier has been realized using oscillator with resonant-inductive degeneration, while drawing 4.8 mA from a 2.2 V supply. The test oscillator achieves a frequency tuning range of 600 MHz, between 5.45–6.05 GHz.**

***Index Terms*—Noise factor, noise folding, phase noise, resonant-inductive degeneration, small-signal loop gain, voltage-controlled oscillator (VCO)**

I. Introduction

In HIGH-PERFORMANCE oscillator circuits, the contribution of the bias current source noise to the phase noise may be larger than all other noise contributions put together (i.e., inductance–capacitance (*LC*)-tank noise and transconductor noise). In particular, converted to the resonator by limiting in the gain stage of the *LC* voltage-controlled oscillator (VCO), the bias current source noise around twice the oscillation frequency has the largest contribution to phase noise around the fundamental.

Therefore, the noise-optimization procedure proposed in this paper is focused on reducing noise generated by the bias current source at twice the oscillation frequency $2f_0$. Resonating a degeneration inductor in the emitter lead of the bias transistor with its base-emitter capacitance at $2f_0$ effectively reduces its output noise that would otherwise be converted into phase noise by hard switching of the oscillator transconductor. We call this "resonant-inductive degeneration" (RID) [1]. It is suitable for low-voltage applications, as it requires no DC voltage headroom. Being in the low-nH range, the resonated bias inductor occupies a relatively small chip area when fabricated using the multiple layers of metal available in modern silicon VLSI technologies. Most importantly, it allows for a manifold phase-noise improvement in *LC*-oscillators.

Manuscript received December 31, 2008; revised April 03, 2009; accepted July 14, 2009. First published December 01, 2009; current version published June 09, 2010.

A. Tasić is with Qualcomm, San Diego, CA 92121 USA (e-mail: atasic@qulcomm.com).

W. A. Serdijn and J. R. Long are with the Electronics Research Laboratory/DIMES, Delft University of Technology, Delft 2628CD, The Netherlands.

Digital Object Identifier 10.1109/TCSI.2009.2030100

The design procedure of the bipolar oscillator with resonant-inductive degeneration is based on the phase-noise model obtained from the spectral noise analysis [2], [3]. This phase-noise model is amenable for design as it describes the noise performance of *LC*-VCOs qualitatively and quantitatively using electrical circuit parameters.

Two bipolar oscillator designs are presented in this paper for the verification of the phase-noise reduction method proposed: one with resonant-inductive degeneration and another without it. At 1 MHz offset from a 5.7 GHz-band carrier (i.e., the upper 802.11a/HIPERLAN/802.16a band [4]–[6]), the oscillator with resonant-inductive degeneration achieves a phase noise of −112 dBc/Hz, while dissipating 10.6 mW. This is a 6 dB improvement in phase noise compared to the *LC*-VCO that does not use resonant-inductive degeneration in the bias current source. Hence, the RID improves noise performance sufficiently to satisfy the phase-noise requirements of 802.11a/HiperLAN/802.16a standards.

This paper is organized as follows. Contributions of all noise sources to the phase noise of bipolar *LC*-oscillators are briefly reviewed in Section II, and the noise factors of the *LC*-tank, transconductor (g_m-cell), and bias current source are formulated. Section III details on the application of the phase-noise model used to improve phase noise in bipolar *LC*-oscillators by means of resonant-inductive degeneration. Results achieved from the resonant-inductive degeneration method are compared with other bias-current source noise reduction techniques in Section IV. Oscillator circuit parameters and experimental results are presented in Section V, confirming the validity of the noise reduction method proposed. Section VI concludes this paper.

II. Phase-Noise Model of Bipolar LC-Oscillators

The VCO shown in Fig. 1 is used for phase-noise analysis of bipolar LC-oscillators. It consists of a resonant *LC* tank, a capacitive voltage divider (C_A, C_B), and a cross-coupled transconductance amplifier (Q_1, Q_2). The bias current source provides current I_{TAIL}. L is the tank inductance, C the tank capacitance, $G_{TK}(1/R_{TK})$ the effective tank conductance.

Noise sources of the oscillator under consideration are also shown in Fig. 1. These are the tank-conductance current noise (symbol i_{GTK} and *rms* value $i_N(G_{TK}) = \sqrt{2KTG_{TK}}$), the base-resistance (r_B) thermal noise (symbol v_B and *rms* value $v_N(r_B) = \sqrt{2KTr_B}$), the collector-current (I_C) shot noise (symbol i_C and *rms* value $i_N(I_C) = \sqrt{KTg_m}$), the base-current (I_B) shot noise (symbol i_B and *rms* value $i_N(I_B) =$

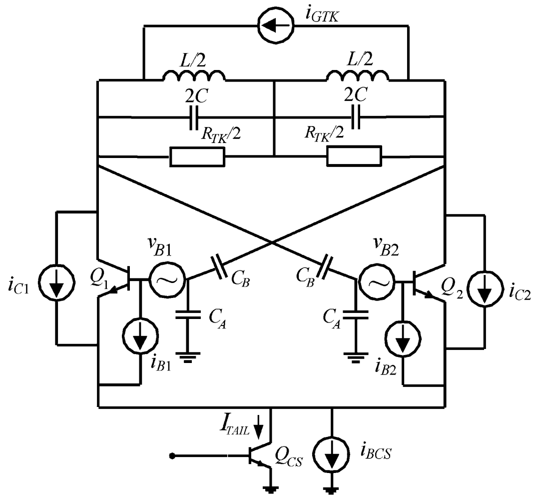

Fig. 1. Bipolar LC-VCO and its main noise sources (bias not completed).

$\sqrt{KTg_m/\beta}$), and the equivalent output current noise (symbol i_{BCS} and *rms* value $i_N(I_{CS})$) of the current source transistor Q_{CS}. T is the absolute temperature, K Boltmann's constant, and β the current gain factor.

A. Noise Factor and Phase Noise of Bipolar LC-Oscillators

The contributions of the oscillator noise source to the phase noise are reviewed in this section [2], [3]. Noise factors of the *LC*-tank loss conductance, g_m-cell collector-current shot noise and base-resistance thermal noise, and bias current source noise are formulated. Finally, the phase-noise model is given, accounting for all the noise contributions.

If we relate the contribution of each noise source *ns* (prior to shaping by the *LC*-tank band-pass characteristic) to phase noise $\mathcal{L}(ns)$ by a noise factor, $F(ns) = v_S^2\mathcal{L}(ns)/4KTG_{TK}$, we obtain the noise factor of the *LC*-tank [2], [3] (i.e., its parallel loss resistance $R_{TK} = 1/G_{TK}$)

$$F(R_{TK}) = 1. \tag{1}$$

v_S stands for the voltage swing across the LC-tank.

Taking into account the contributions of the collector-current shot-noise sources from both transconductor transistors, a noise factor $F(2I_C)$ is obtained [2], [3]

$$F(2I_C) = \frac{n}{2} \tag{2}$$

where n stands for the capacitive divider ratio $n = 1 + (C_A + C_\pi)/C_B, C_\pi$ being a base-emitter capacitor of the g_m-cell transistors. This result suggests that the phase-noise contribution of the g_m-cell collector-current shot-noise is independent of the small-signal loop gain and power consumption, but depends on n only.

The base-resistance thermal noise $v_N(r_B)$ components at around odd multiples of resonant frequency fold to the resonator via the even-order harmonic components of the small-signal time-varying gain of the g_m-cell [2], [3]. Taking into account both transistors of the g_m-cell, the total base-resistance phase-noise contribution is given by a noise factor $F(2r_B)$ of (3) [2], [3]

$$F(2r_B) = \frac{2}{3}nkc \tag{3}$$

where $c = r_B g_{m-SUP}$ is the start-up constant, $g_{m-SUP} = 2nG_{TK}$ the start-up transconductance of the g_m-cell transistors, $k = g_m/(2nG_{TK})$ the small-signal loop gain, and g_m the transconductance of bipolar transistors Q_1, Q_2.

This result suggests that the contribution of the g_m-cell base-resistance noise to the phase noise of the oscillator under consideration is directly proportional to the small-signal loop gain k (thus power consumption) and the parameters n and c, the latter relating the base resistance of the transconductor transistors and the quality of the resonator.

Folding of the bias current source noise is a result of operation of the g_m-cell in the limiting region (i.e., a result of a large oscillation signal generated). The transconductor switching function converts the bias current source noise from around even multiples of the oscillation frequency back to the *LC*-tank at around the oscillation frequency f_0.

The resulting noise factor of the bias current source $F(I_{BCS})$ is given as follows [2], [3]:

$$F(I_{BCS}) = k\left(\frac{n}{2} + nkc\right). \tag{4}$$

Without loss of generality, we have used for a bias current source transistor transconductance $g_{m,CS} = 2g_m$ and assumed $2r_{B,CS} = r_B$, given the same transit frequencies (f_T) of transistors Q_1, Q_2 and Q_{CS} (thus, Q_{CS} twice as large as Q_1, Q_2 is assumed). Index $_{CS}$ refers to bias current source transistor Q_{CS}.

Assumed to be uncorrelated, all noise sources, viz., the tank conductance noise, the transconductor base resistance thermal noise and current shot noise, and the bias current source noise, add up to an equivalent phase-modulating noise component. With the aid of (1)–(4), the noise factor of the bipolar LC-oscillator now becomes as given by (5) and (6)

$$F = F(R_{TK}) + F(2I_C) + F(2r_B) + F(I_{BCS}) \tag{5}$$

$$F = 1 + (1+k)\frac{n}{2} + \left(\frac{2}{3} + k\right)nkc. \tag{6}$$

The oscillator phase noise defined as the ratio of the noise power in a 1 Hz bandwidth at frequency $f_0 + \Delta$ and the carrier power at frequency f_0 now reads [2], [3], [7]

$$\begin{aligned}\mathcal{L} &= \frac{4KTG_{TK}F}{v_S^2(4\pi C_{\mathrm{TOT}}\Delta)^2}\\ &= 4KTG_{TK}\frac{F(R_{TK}) + F(2I_C) + F(2r_B) + F(I_{BCS})}{v_S^2(4\pi C_{\mathrm{TOT}}\Delta)^2}\end{aligned} \tag{7}$$

where C_{TOT} for the total capacitance across the *LC*-tank. Substituting (6) into (7), the phase noise finally becomes [2], [3]

$$\mathcal{L} = \frac{4KTG_{TK}}{(4\pi C_{\mathrm{TOT}}\Delta)^2}\left(\frac{\pi}{8V_T}\right)^2\frac{1 + (1+k)\frac{n}{2} + \left(\frac{2}{3} + k\right)nkc}{k^2n^2}. \tag{8}$$

where we have used $v_S = 8\,knV_T/\pi$ [2], with V_T being bipolar transistor thermal voltage.

The result obtained is a fundamental description of the phase-noise phenomenon in the *LC*-oscillator under consideration. The model developed doesn't require use of numerical solvers, yet providing oscillator designers with a valuable tool for analysis and synthesis of high-performance oscillators.

The phase-noise model is parameterized with respect to current consumption via the small-signal loop gain k [2] that can be varied by $I_{\rm TAIL}$ shown in Fig. 1. Parameter k also defines the excess negative conductance necessary to compensate the losses in the *LC*-tank (i.e., G_{TK}).

It is important to note that (6) is the worst-case noise factor of the bipolar oscillator under consideration, thereby overestimating its phase noise as given by (8). The small-signal loop-gain related contributions, viz., the base-resistance noise contribution of the transconductor, (3), and the base-resistance and collector-current noise contributions of the bias current source, (4), are calculated implicitly assuming infinite bandwidth of both the noise sources and the operation of the oscillator devices. However, the results obtained are intuitive and describe qualitatively the rather complex phase-noise generating mechanism in *LC*-oscillators. The formulations derived are amenable for design as they describe the oscillator phase-nose performance using electrical parameters.

B. Implications of the Phase-Noise Model on Oscillator Design

To compare the contribution of the bias current source noise and other noise sources to phase noise of oscillators, we introduce the phase-noise ratio (*PNR*). It is the ratio of phase noise of oscillators with and without the contribution of the bias current source noise. For a bipolar LC-VCO shown in Fig. 1, the *PNR* is given by (9)

$$\begin{aligned} PNR &= \frac{F(R_{TK}) + F(2I_C) + F(2r_B) + F(I_{BCS})}{F(R_{TK}) + F(2I_C) + F(2r_B)} \\ &= 1 + \frac{k\left(\frac{n}{2} + nkc\right)}{1 + \frac{n}{2} + \frac{2}{3}nkc} \cong 1 + k\frac{F(2I_C, 2r_B)}{1 + F(2I_C, 2r_B)} \end{aligned} \tag{9}$$

where $F(2I_C, 2r_B)$ is the noise factor of the g_m-cell. Equation (9) shows that failing to suppress the noise contribution of the bias current source (BCS) to the phase noise, a factor in the order of k degraded performance results. For example, for a typical small-signal loop gain of $k \sim 10$, calculations suggest a degradation of the phase noise of $\sim$10 dB due to the contribution of the bias current source noise, even for a high-quality *LC*-tank designed.

To confirm these findings, the oscillator shown in Fig. 1 is simulated using SpectreRF with the following parameters (extracted from the layout [1]): oscillation frequency f_0 $\sim$5.74 GHz, tank resistance R_{TK} $\sim$ 340 Ω, capacitive divider ratio n $\sim$ 1.6, start-up constant c $\sim$ 0.25, supply voltage $V_{CC} = 2.2$ V.

The *PNR* of (9) is compared with the simulation results as shown in Fig. 2, taking into account the relationship between the calculated and simulated small-signal loop gain. At the maximum small-signal loop gain of around 10, the noise from the BCS degrades the phase noise of the oscillator under consideration by 8.2 dB in the simulations (8.7 dB calculated), as already presumed. The overwhelming contribution of the BCS noise to the phase noise is also visualized in Fig. 3. For a small-signal loop gain of around 10, the bias current source noise accounts for around 85%, the g_m-cell noise for around 10%, and the *LC*-tank noise for 5% of the phase-related noise power. The noise sources considered account for around 90% of the total phase noise, as obtained from the simulations.

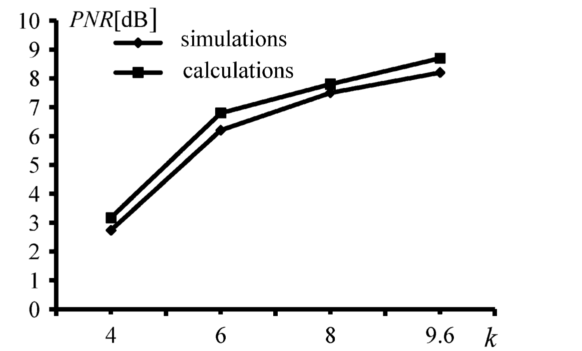

Fig. 2. Calculated versus simulated phase-noise ratio for a bipolar *LC*-oscillator.

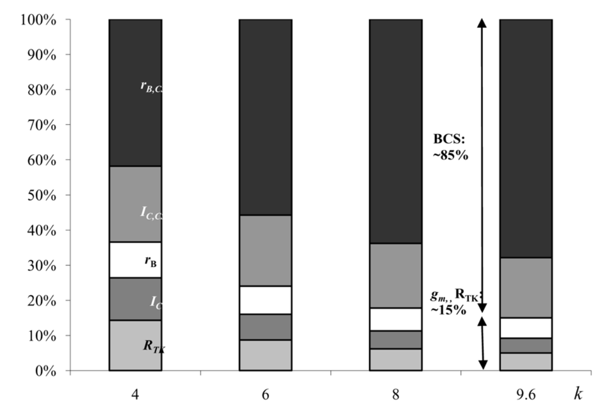

Fig. 3. Simulated bipolar *LC*-oscillator phase-noise contributions, normalized to 100%.

III. Resonant-Inductive Degeneration

It has been shown in the previous section that the contribution of noise from the bias current source to the phase noise of the *LC*-oscillator considered is larger than all other noise contributions combined. In particular, the BCS noise around twice the oscillation frequency has the largest contribution [1].

We introduce resonant-inductive degeneration [1] as a design procedure to minimize the noise contribution of the oscillator bias current source. It relies on forming a resonance between the inductor (L_{RID}) in the emitter of the bias current source transistor Q_{CS} and its base-emitter capacitance $C_{\pi,CS}$ at twice the oscillation frequency $2f_0$, as shown in Fig. 4(a). The fact that the bias current source noise around $2f_0$ has the largest contribution to the phase noise of the oscillator, after being converted to the resonating *LC*-tank by the switching of transconductor Q_1-Q_2 (see Fig. 1), stems for the resonant frequency chosen.

The resonant-inductive degeneration results in reduction of the contributions of the base-resistance thermal noise and collector-current shot noise of the BCS to the oscillator phase noise. The high impedance in the emitter of Q_{CS} at resonance reduces its transconductance and accordingly the gain from its base-resistance thermal noise to the output, and impedes the flow of its collector-current shot noise, making these noise contributions negligible.

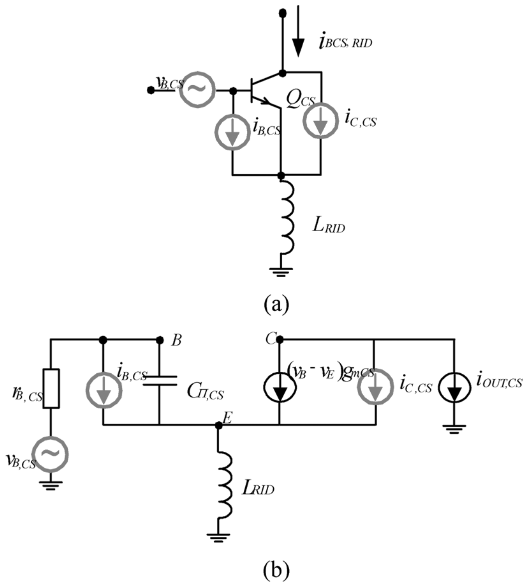

Fig. 4. (a) Resonant-inductive degenerated bias current source transistor and its noise sources, (b) detailed schematic of the degenerated bias current source.

We will determine the performance of resonant-inductive degeneration by calculating the transfer functions from the base-resistance noise, base-current shot noise, and collector-current shot noise sources to the output of the bias current source using a detailed schematic shown in Fig. 4(b). Then, using superposition, the total output noise of the bias current source with resonant-inductive degeneration will be determined, and new formulations for the oscillator noise factor and phase noise provided.

Fig. 4(b) shows the base-resistance noise source $v_{B,CS}$, base-current shot noise source $i_{B,CS}$, and collector-current shot-noise source $i_{C,CS}$ of the BCS transistor. $i_{\mathrm{OUT},CS}$ models the total output current source noise of the BCS to be determined. The corresponding double-sided noise densities are given by (10)–(12)

$$v_N^2(r_{B,CS}) = 2KTr_{B,CS} \tag{10}$$
$$i_N^2(I_{C,CS}) = qI_{\mathrm{TAIL}} = 2KTg_{m,CS}/2 \tag{11}$$
$$i_N^2(I_{B,CS}) = qI_{B,CS} = 2KTg_{m,CS}/(2/\beta). \tag{12}$$

A. Transformation of the Base-Resistance Noise of the Resonant-Inductive Degenerated Bias Current Source

The circuit of Fig. 4(b) resembles the circuit of an inductively-degenerated low-noise amplifier. Unlike a low-noise amplifier, where noise at the input of a degenerated transistor is minimized, for a bias current source, the minimum of noise at the output of a degenerated transistor matters.

The input impedance of an inductively degenerated transistor is given by [2], [8]

$$Z_{\mathrm{IN}}(f) = 2\pi f_{T,CS}L_{RID} + j\left[2\pi f L_{RID} - \frac{f_{T,CS}}{f}\frac{1}{g_{m,CS}}\right] \tag{13}$$

where $f_{T,CS}$ is the transit frequency of Q_{CS}. The contribution of the noise from the base resistance to the output current noise density $i_{\mathrm{OUT},CS}$ of the degenerated bias current source can be calculated from [1], [2] as

$$\begin{aligned}\frac{i_{\mathrm{OUT}}}{v_N(r_{B,CS})}(f) &= -\frac{1}{Z_{\mathrm{IN}}(f)}\frac{\omega_{T,CS}}{\omega} \\ &= \frac{-1}{\omega_{T,CS}L_{RID} + j\omega L_{RID} + 1/(j\omega C_{\Pi,CS})}\frac{\omega_{T,CS}}{\omega}.\end{aligned} \tag{14}$$

For the resonance at $2f_0$, the imaginary part of the input impedance is set to zero. Then

$$R_{\mathrm{IN}}g_{m,CS} = \left(\frac{f_{T,CS}}{2f_0}\right)^2 \tag{15}$$

where $R_{\mathrm{IN}} = 2\pi f_{T,CS}L_{RID}$ is equal to the real part of the impedance at the base of Q_{CS} at resonance.

From (14), the equivalent transconductance of the RID bias current source transistor at $2f_0$ now equals [1], [2]

$$g_{EQ,CS} \cong -\frac{1}{R_{\mathrm{IN}}}\frac{f_{T,CS}}{2f_0} \tag{16}$$

and (14) becomes

$$\frac{i_{\mathrm{OUT},CS}}{v_N(r_{B,CS})}(2f_0) = -g_{m,CS}\frac{2f_0}{f_{T,CS}}. \tag{17}$$

This suggests that the bias current source base-resistance thermal noise can be reduced for $2f_0/f_{T,CS} < 1$. It is interesting to note that seen from base of the transistor Q_{CS}, inductor L_{RID} and base-emitter capacitor $C_{\pi,CS}$ form a series-resonant circuit (see the denominator of (14)).

B. Transformations of the Base- and Collector-Current Shot Noise Sources of the Resonant-Inductive Degenerated BCS

The RID bias current source transistor Q_{CS} operates in a common-base-like configuration rasonating at twice the oscillation frequency. Referred to the output of transistor Q_{CS}, we expect to see the collector-current shot noise suppressed and the base-current shot noise present. This intuitive observation can be analytically proved with the aid of Fig. 4(b). We will first determine the transfer function for collector-current shot noise $i_{C,CS}$ to the output of the current source $i_{\mathrm{OUT},CS}$ by applying superposition (i.e., $i_{B,CS} = 0$ and $v_{B,CS} = 0$).

Let us first find the gain from $i_{C,CS}$ to $i_{\mathrm{OUT},CS}$. Kirchoff's current law equation for node E yields

$$i_{C,CS} + g_{m,CS}v_{BE} = \frac{v_E}{j\omega L_{RID}} - j\omega C_{\Pi,CS}v_{BE} \tag{18}$$

where $v_{BE} = v_B - v_E$. Analyzing the BE branch of Fig. 4(b), we obtain

$$\frac{v_E}{r_{B,CS}} = -v_{BE}\left(\frac{1}{r_{B,CS}} + j\omega C_{\Pi,CS}\right). \tag{19}$$

Substituting (18) into (19), the relationship between the base-emitter voltage v_{BE} and the current $i_{C,CS}$ becomes

$$i_{C,CS} = -v_{BE}\left[g_{m,CS} + j\omega C_{\Pi,CS} + \frac{1}{j\omega L_{RID}} + \frac{C_{\Pi,CS} r_{B,CS}}{L_{RID}}\right]. \quad (20)$$

From the current-law equation for node C,

$$i_{\mathrm{OUT},CS} = i_{C,CS} + g_{m,CS} v_{BE} \quad (21)$$

the transfer function from the collector-current noise source to the output of the BCS is

$$\frac{i_{\mathrm{OUT},CS}}{i_N(I_{C,CS})}(f) = 1 - \frac{g_{m,CS}}{g_{m,CS} + \frac{C_{\Pi,CS} r_{B,CS}}{L_{RID}} + j\omega C_{\Pi,CS} + \frac{1}{j\omega L_{RID}}}. \quad (22)$$

At the resonance $(2f_0)$ between L_{RID} and $C_{\pi,CS}$, this simplifies to

$$\frac{i_{\mathrm{OUT},CS}}{i_N(I_{C,CS})}(2f_0) = 1 - \frac{1}{1 + r_{B,CS} g_{m,CS}\left(\frac{2f_0}{f_{T,CS}}\right)^2} \cong 0. \quad (23)$$

As $r_{B,CS} g_{m,CS}$ is a small constant (equals ck for $2r_{B,CS} = r_B$) and $2f_0/f_{T,CS} \ll 1$, it can be seen that the collector-current shot noise can be suppressed to a large extent from the output of the BCS.

In a similar manner, the transformation of the base-current shot noise to the output of the BCS is calculated from Fig. 4(b) ($i_{C,CS} = 0$ and $v_{B,CS} = 0$). The resulting transfer function reads

$$\frac{i_{\mathrm{OUT},CS}}{i_N(I_{B,CS})}(f) = \frac{g_{m,CS}}{g_{m,CS} + \frac{C_{\Pi,CS} r_{B,CS}}{L_{RID}} + j\omega C_{\Pi,CS} + \frac{1}{j\omega L_{RID}}} \quad (24)$$

or at $2f_0$

$$\frac{i_{\mathrm{OUT},CS}}{i_{B,CS}}(2f_0) = \frac{1}{1 + r_{B,CS} g_{m,CS}\left(\frac{2f_0}{f_{r,CS}}\right)^2} \cong 1. \quad (25)$$

This implies that the base-current shot noise is transferred completely to the output of the degenerated bias current source.

It is worth mentioning that the inductor L_{RID} and base-emitter capacitor $C_{\pi,CS}$ form a parallel-resonant circuit as seen from the base- and collector-current noise sources (see the denominators of (22) and (24)). Thus, the very same reactive components appear to resonate in series and parallel when referred to from different terminals of the degenerated current source transistor.

C. Total Output Noise and Noise Factor of the Resonant-Inductive Degenerated Bias Current Source

Combining the base-resistance noise and base-current shot noise contributions, (17) and (25) (contribution of the collector-current shot noise close to zero), the total output current noise density of the resonant-inductive degenerated bias current source becomes

$$i_N^2(I_{BCS,RID}) = kT g_{m,CS} \times \left[0 + \left(\frac{f_{T,CS}}{2f_0}\right)^2 \frac{1}{\beta} + 2r_{B,CS} g_{m,CS}\right]\left(\frac{2f_0}{f_{T,CS}}\right)^2. \quad (26)$$

The noise factor of the bias current source with resonant-inductive degeneration now equals

$$F(I_{BCS,RID}) = k \cdot \left[\frac{n}{2\beta}\left(\frac{2f_{T,CS}}{f_0}\right)^2 + nkc\right]\left(\frac{2f_0}{f_{T,CS}}\right)^2 \quad (27)$$

which is obtained with the aid of (4) and (26), again after referring to $2r_{B,CS} = r_B$ for a convenient formulation.

In order to estimate the improvement achieved, (26) is compared to the output current noise density of the BCS without degeneration, given by (28) [1]

$$i_N^2(I_{BCS}) = 2KT\frac{g_{m,CS}}{2} \times \left[1 + 0 \cdot \left(\frac{f_{T,CS}}{2f_0}\right)^2 \frac{1}{\beta} + 2r_{B,CS} g_{m,CS}\right]. \quad (28)$$

A comparison between (26) and (28) suggests that by applying resonant-inductive degeneration, the contribution of the bias current source noise is reduced more than $(f_{T,CS}/2f_0)^2$

$$F(I_{BCS,RID}) < \left(\frac{2f_0}{f_{T,CS}}\right)^2 F(I_{BCS}) \quad (29)$$

as it can be assumed that the current gain factor $\beta > (f_{T,CS}/(2f_0))^2$.

For example, a factor 25 reduction of the BCS noise is possible for $f_{T,CS} = 10f_0$. Minimizing or eliminating the noise contribution of the BCS improves the phase noise performance of the oscillator, or permits operation at a lower bias current for the same performance of the oscillator under consideration.

Resonant-inductive degeneration suppresses most effectively the bias current noise around second harmonic of the oscillation frequency by forming a resonance, but also the BCS noise from higher harmonics $(4f_0, 6f_0, \ldots)$. The BCS noise around $2f_0$ is responsible for around 72% [1] of the total bias noise, which is reduced by a factor $(f_{T,CS}/2f_0)^2$ after RID. The smaller portion of the BCS noise ($\sim$ 28%) originates from higher harmonics, which is reduced by forming a high impedance in emitter of the BCS transistor ($\sim 4\omega_0 L_{RID}$ at $4f_0, 6\omega_0 L_{RID}$ at $6f_0, \ldots$), that is, the gain for the thermal base-resistance noise to the output of the BCS is small and the flow of collector-current shot noise impeded for higher harmonics. This allows us to formulate the noise factor for the RID BCS by (27).

Before closing this section, let us inspect (26) and (28) from another perspective. Whereas the base- and collector-current shot noise contributions of the bias current source are fixed by the supply current, the base-resistance thermal noise is determined by transistor dimensions ($r_{B,CS}$ is inversely proportional to length l of the transistor). Therefore, for a BCS without degeneration, we opt for a large bias transistor in order to reduce $r_{B,CS}$ and the contribution of the base-resistance noise, as suggested by (28).

However, for a BCS with the RID, it is not $r_{B,CS}$, but the ratio $r_{B,CS}/f_{T,CS}^2$ that matters, as implied by (26). As $r_{B,CS} \sim 1/l$ and, for a given current consumption, $f_{T,CS} \sim 1/l$, the ratio $r_{B,CS}/f_{T,CS}^2 \sim l$. Thus, for the BCS with the RID, we opt for a small transistor, which provides a larger transition frequency at a given bias current I_{TAIL}. These findings stress the opposing requirements on the design of a bias current source with and without degeneration.

Although the contribution of the bias current source noise to the phase noise in CMOS *LC*-oscillators can be made small by trading off bias current, transistors size, and overdrive voltage, the resonant-inductive degeneration can still be effectively applied if, for example, the CMOS *LC*-oscillator transistors operate in weak inversion.

D. Noise Factor and Phase Noise of Oscillators With Resonant-Inductive Degeneration

The noise factor of the bipolar LC oscillator with resonant-inductive degenerated bias current source is now obtained with the aid of (5), accounting for the reduction of the BCS noise achieved (see (27)). The noise factor reads

$$F = 1+\frac{n}{2}+\frac{2}{3}nkc+k\cdot\left[\frac{n}{2\beta}\left(\frac{2f_{T,CS}}{f_0}\right)^2+nkc\right]\times\left(\frac{2f_0}{f_{T,CS}}\right)^2 \tag{30}$$

or in the worst case (assuming $\beta = (f_{T,CS}/(2f_0))^2$)

$$F \cong 1+\frac{n}{2}+\frac{2}{3}nkc+k\left(\frac{n}{2}+nkc\right)\left(\frac{2f_0}{f_{T,CS}}\right)^2. \tag{31}$$

For $2f_0/f_{T,CS} \ll 1$, which is readily achievable, the BCS noise contribution can be eliminated, whereby the noise factor of the *LC*-oscillator with an RID BCS becomes

$$F \cong 1+\frac{n}{2}+\frac{2}{3}nkc. \tag{32}$$

In this case, the phase noise of the LC oscillator of Fig. 1 with a bias current source of Fig. 4 is

$$\mathcal{L} = \frac{4KTG_{TK}}{(4\pi C_{\text{TOT}}\Delta)^2}\left(\frac{\pi}{8V_T}\right)^2\frac{1+\frac{n}{2}+\frac{2}{3}nkc}{n^2k^2}. \tag{33}$$

Now the discussion of Section II-B becomes more apparent. Namely, for a high-performance *LC*-tank designed ($c \ll 1$), the phase noise of a bipolar *LC* oscillator with a common-emitter bias transistor is proportional to $1/k$, given $k \gg 1$ (see (8)). However, biasing the same oscillator circuit with a resonant inductor-degenerated transistor, the phase noise becomes proportional to $1/k^2$ [see (33)], a factor k improvement.

E. Verification of the Resonant-Inductive Degeneration Phase-Noise Reduction Method

The phase-noise ratio for the oscillator biased from the BCS (see Fig. 1) and the oscillator biased from the resonant-inductive degenerated BCS (Fig. 1 with bias circuit of Fig. 4) is given by (34)

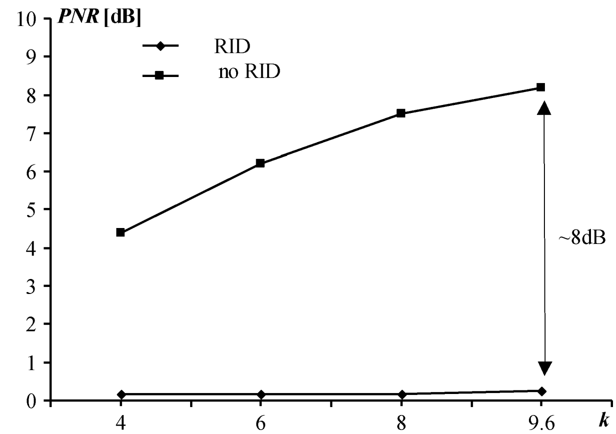

Fig. 5. Phase-noise ratio before and after resonant-inductive degeneration (noise contributions considered are normalized to 100%).

$$\begin{aligned} PNR &= \frac{F(R_{TK})+F(2I_C)+F(2r_B)+F(I_{BCS,RID})}{F(R_{TK})+F(2I_C)+F(2r_B)} \\ &\cong 1+k\left(\frac{2f_0}{f_{T,CS}}\right)^2\frac{F(2I_C,2r_B)}{1+F(2I_C,2r_B)} \end{aligned} \tag{34}$$

This is a ratio of the oscillator phase noise with and without the contribution of the noise from the RID bias current source. As implied by (34), applying the resonant-inductive degeneration method, a manifold reduction of the bias current source noise can be achieved, thereby improving the phase noise of the oscillator under consideration. For $2f_0/f_{T,CS} < 1$, (34) results in $PNR \sim 1$ (~0 dB), that is, the phase-noise contribution of the BCS noise becomes negligible.

For the oscillator parameters given in Section II-B, the *PNR* of the oscillator with resonant-inductive degeneration ($L_{RID} =$ 1.3 nH) applied to the biasing current source has been simulated [see (34)], and the results compared to the *PNR* of the oscillator biased from the BCS without any degeneration [see (9)]. As shown in Fig. 5, simulations show an improvement of around 8 dB in phase noise, at a small-signal loop gain of around 10, as predicted by (34). This result verifies the resonant-inductive degeneration noise-reduction method.

The contribution of the BCS noise to the phase noise after the RID is applied to the bias current source is visualized by Fig. 6. At a small-signal loop gain of around 10, the BCS noise accounts for around 6%, the g_m-cell noise for around 64%, and the *LC*-tank noise for 30% of the phase-related noise power. A considerable improvement has been achieved: the contribution of the BCS noise to the phase noise has been reduced from 85% for the oscillator *without* the RID (see Fig. 3) to only 6% for the oscillator *with* the RID applied.

IV. Comparison of Resonant-Inductive Degeneration With Other Bias-Current Source Noise-Reduction Methods

Pros and cons of the resonant-inductive degeneration are summarized in this section and its performance compared to other bias-current source noise reduction techniques known:

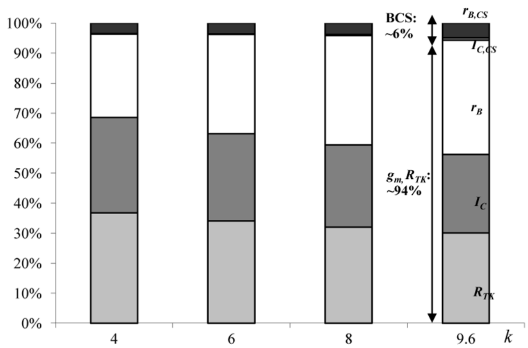

Fig. 6. Simulated *LC*-oscillator phase-noise contributions after resonant-inductive degeneration, normalized to 100%.

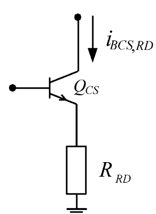

Fig. 7. Resistive-degenerated bias current source.

resistive degeneration, capacitive and capacitive-inductive filtering, and inductive degeneration are considered.

A. Advantages of Resonant-Inductive Degeneration

Resonant-inductive degeneration suppresses most effectively bias current-source noise in bipolar *LC*-oscillators around second harmonic of the oscillation frequency by forming a resonance, but also the BCS noise from higher harmonics.

This noise reduction method is suitable for low-voltage applications, as it requires no DC voltage headroom. Moreover, the RID inductor is in the low-nH range for GHz-range applications and, as such, occupies a relatively small chip area when fabricated using the multiple layers of metal available in modern silicon VLSI technologies.

B. Resistive Degeneration of Bias Current Source

Resistive degeneration [2], [9] of a bias current source suppresses its noise equally at all frequencies, opposite to RID that is frequency selective. Merit of resistive degeneration is in the suppression of the low-frequency noise, which is otherwise converted to the resonator and then to phase noise via AM-to-FM conversion in the *LC*-tank varactor [10].

However, as the resistor in the emitter of the BCS transistor requires some DC voltage headroom, this method of noise suppression has limited use to systems with large supply voltages (e.g., > 3 V).

The circuit diagram of the resistive degenerated (RD) BCS is shown in Fig. 7. The performance of this noise-reduction method is discussed next.

The collector-current shot noise of the resistively-degenerated BCS is suppressed while the base-current shot noise is transferred to the output of the current source, as has been the case with the RID BCS. Moreover, the base-resistance and the degenerative-resistor (R_{RD}) noise sources are transferred to the output of the current-source transistor with the equivalent transconductance $g_{EQ,CS} = 1/R_{RD}$, assuming $g_{m,CS}R_{RD} \gg 1$.

Accounting for the contributions of the base-resistance noise, base-current shot noise, and degenerative resistance noise, the output current-noise density of the RD BCS equals

$$\begin{aligned} i_N^2(I_{BCS,RD}) &= 2KT\frac{g_{m,CS}}{2} \\ &\times \left[\frac{1}{\beta} + 2r_{B,CS}\frac{1}{g_{m,CS}R_{RD}}\left(\frac{1}{r_{B,CS}} + \frac{1}{R_{RD}}\right)\right]. \end{aligned} \quad (35)$$

For a realistic assumption $R_{RD} \gg r_{B,CS}$, this becomes

$$i_N^2(I_{BCS,RD}) = 2KT\frac{g_{m,CS}}{2}\left[\frac{1}{\beta} + \frac{2}{g_{m,CS}R_{RD}}\right]. \quad (36)$$

This result can now be directly compared to the total output current noise density of the RID BCS (26). The resonant-inductive degeneration is more effective than the resistive degeneration, if condition (37) is satisfied

$$\left(\frac{f_{T,CS}}{2f_0}\right)^2 \frac{1}{r_{B,CS}g_{m,CS}} > g_{m,CS}R_{RD}. \quad (37)$$

As $r_{B,CS}g_{m,CS}$ is a small constant (equals c for Q_{CS} 2 times larger than Q_1, Q_2) and $2f_0/f_{T,CS} \ll 1$, resonant-inductive degeneration can be considered as a better solution than resistive degeneration for low-supply voltages (e.g., $V_{CC} < 3$ V) and the oscillator under consideration. For example, for $c \sim 0.1$ (typical for high-performance *LC*-tanks), and $f_{T,CS} = 10f_0$, the resistive degeneration would not be the noise reduction method of choice, as an impractically large loop gain $(g_{m,CS}R_{RD} > 250)$ around the RD transistor would be required, given a low supply voltage.

However, if a high supply voltage were available, resistive degeneration would be preferable, as its implementation is rather straightforward.

C. Capacitive Filtering Technique

By placing a capacitor in parallel with the BCS transistor, the output bias current-source noise is filtered over a range of frequencies [11]. However, as much as the capacitor suppresses the BCS noise, it enlarges the noise contribution of the oscillator transconductor, thereby partly counteracting the complete effectiveness. The reason for this is the low impedance generated by the capacitive AC short at the emitters of the g_m-cell transistors at the fundamental frequency. To better understand the effect of such an AC short on the phase noise, a schematic of the oscillator g_m-cell in the limiting region (Q_1 is on and Q_2 is off) is shown in Fig. 8, depicting the spliting of the collector-current shot noise source.

In the limiting region of the g_m-cell, when only Q_1 (or Q_2) is active, the collector-current shot-noise source, i_{C1} in Fig. 8(a), flows completely through one half of the *LC*-tank, as shown in Fig. 8(b). Thus, collector-current shot noise contributes to the phase-modulating noise component of the oscillator not only in the linear region, but also in the limiting region of the g_m-cell, failing to provide high impedance at collector of the BCS transistor. Shown in Fig. 9(a) is the gain from collector-current shot

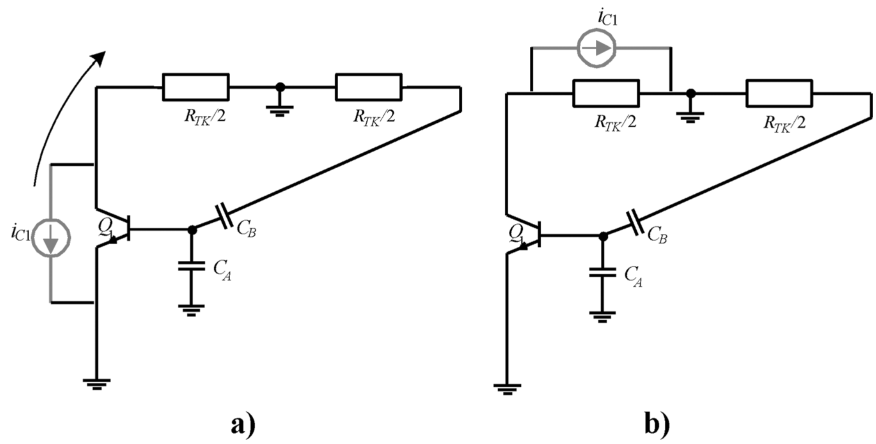

Fig. 8. Splitting of the g_m-cell collector-current shot noise in the limiting region for the g_m-cell emitter AC shorted at f_0: (a) noise source across Q_1, (b) noise source across *LC*-tank.

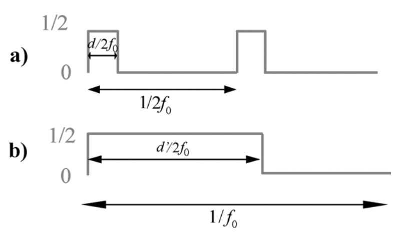

Fig. 9. Time-varying gain from the g_m-cell collector-current shot-noise sources: (a) high BCS output impedance, (b) low BCS output impedance (AC short at f_0).

noise source to the resonator for a high BCS output impedance, and in Fig. 9(b) for a low BCS output impedance (time-varying gain for both shot-noise sources are the same, but time-delayed).

Thus, while suppressing BCS noise with the capacitive filtering, the relative collector-current shot noise contribution (i.e., noise contribution time per period) of both transconductor transistors to phase noise is $1/2 + d/2$ instead of d without filtering employed, d being the duty cycle of the g_m-cell small-signal time-varying gain [2], [3]. That is, for $d \ll 1$, a larger collector-current shot noise portion contributes to the phase noise of the oscillator $(1/2 + d/2 \gg d)$.

Let us now analytically describe these observations, aided by intuition and experience gained from the previous sections and [1]–[3].

Given a duty cycle $d = 1/(2k)$, the phase-modulating noise component originating from the transconductor collector-current shot-noise source equals [2], [3]

$$i_{PM}^2(I_C) = d\frac{i_N^2(I_C)}{2}. \tag{38}$$

If we denote a duty cycle of the gain function shown in Fig. 9(b) as d', we can use (38) modified for the new value d' to express the phase-modulating noise component from the transconductor collector-current shot noise $i'_{PM}(I_C)$. This is given by (39) and (40)

$$d' = \frac{1}{2}(1 + d) \tag{39}$$

$$i_{PM}^{\prime 2}(I_C) \cong d'\frac{i_N^2(I_C)}{2}. \tag{40}$$

Combining the contributions from both transistors, the g_m-cell collector-current shot-noise factor $F'(2I_C)$ for a capacitively-filtered BCS noise now equals

$$F'(2I_C) \cong \frac{4i_{PM}^{\prime 2}(I_C)}{4KTG_{TK}} = \frac{n}{2}\left(\frac{1}{2} + k\right) > F(2I_C). \tag{41}$$

While the BCS noise contribution is reduced, the contribution of the g_m-cell collector-current shot noise to the phase noise tends to increase, as suggested by (41). For example, for $k \gg 1$, a degradation of the phase noise performance may result from the capacitive filtering when compared to the resonant-inductive degeneration phase-noise reduction method.

D. Capacitive-Inductive Filtering Technique

In addition to a capacitor in parallel with the BCS, an inductor is placed between the current source and the oscillator core in [12]. This solves the problem of an AC short generated by the capacitive filtering at the collector of the BCS transistor.

We emphasize two interesting points of this technique. First, a large capacitor, occupying a large area, is required for a good suppression of the BCS noise. Second, the output impedance of the capacitively-inductively filtered BCS is smaller then that of the RID BCS. In the former, the output impedance is the impedance of the inductor L_E at collector of the BCS transistor $Z_{\mathrm{OUT}}(L_E)$, (42), whereas in the latter it is the impedance of the emitter degenerated transistor $Z_{\mathrm{OUT}}(L_{RID})$, (43) [13]

$$|Z_{\mathrm{OUT}}(L_E)| = \omega L_E \tag{42}$$

$$|Z_{\mathrm{OUT}}(L_{RID})| > g_{m,CS} r_{O,CS} \omega L_{RID}. \tag{43}$$

Given a large output resistance of the bipolar BCS transistor $r_{O,CS}$, $Z_{\mathrm{OUT}}(L_{RID})$ is larger than $Z_{\mathrm{OUT}}(L_E)$. Or, in other words, a few orders of magnitude larger inductor L_E is needed for $Z_{\mathrm{OUT}}(L_E) = Z_{\mathrm{OUT}}(L_{RID})$.

Therefore, a better suppression of the g_m-cell noise in the limiting region can be expected with resonant-inductive degeneration of the bias current source.

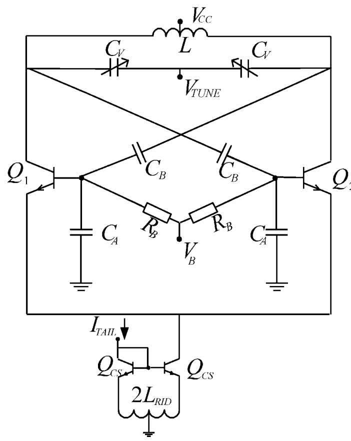

Fig. 10. Bipolar *LC*-VCO with resonant-inductive degenerated bias current source.

E. Inductive Degeneration

Another way to reduce the bias current source output noise is to apply inductive degeneration [14]. However, a large discrete inductor in order of uH used may pick some external noise and additionally degrade the oscillator phase-noise performance. We have shown that an inductance value in the order of nH, resulting from the *resonant inductive degeneration* method proposed in this paper, allows for almost complete removal of the bias current-source noise, yet amenable for integration on chip.

V. Test Oscillator Designs

Two test oscillators have been designed for the verification of the phase-noise reduction method introduced, both operating in the upper 5 GHz band.

A schematic of the test circuit of a bipolar *LC*-VCO designed with the resonant-inductive degeneration applied to its bias current source is depicted in Fig. 10. Shown are the symmetric *LC*-tank inductor L, two nMOS varactors C_V, feedback capacitors C_A and C_B, a cross-coupled transconductor (Q_1-Q_2), and a bias current source transistor Q_{CS} with a resonant degenerative inductor L_{RID}. V_{CC} is the supply voltage, $V_{\rm TUNE}$ the varactor tuning voltage, V_B the base bias voltage, and $I_{\rm TAIL}$ the bias tail current.

Another (identical) voltage-controlled oscillator has been designed without resonant-inductive degeneration, for validation of the noise-reduction method proposed. The two oscillator designs have identical *LC*-tanks, transconductors, and bias current source transistors. The only difference between the two oscillators is that $L_{RID} = 0$ for the oscillator without RID.

A. Oscillator Circuit Parameters

The test oscillators bias and circuit parameters are optimized for the largest voltage swing around the 5.7 GHz central oscillation frequency.

For a supply voltage of 2.2 V, a transconductor base bias voltage V_B between 1.8–1.85 V has been chosen. It allows for both the largest voltage swing of the output signal and the most efficient use of the voltage headroom available, as obtained from the simulations. The maximum voltage swing is estimated from the saturation condition of the transconductor transistors, in order to avoid noise injection of the forward-biased base-collector junctions [15]. For a capacitor divider ratio or around $n \sim$ 1.6, a maximum voltage swing across the bases of the transconductor $v_{S,B}$ of around 0.68 V is expected, corresponding to a small-signal loop gain of around 10.

For suppression of the bias current source noise at twice the oscillation frequency (i.e., between 11 GHz and 12 GHz), a symmetric low-quality resonant-degenerative inductor of 2.6 nH $(2L_{RID})$ was integrated in 1.25 um thick metal. It has 7 turns, outer diameter of 106 um, metal width of 5 um, and metal spacing of 1.5 um. A small resistor (30 Ω) was added in series with the degenerative inductor. Although this has minor effect on high-frequency bias current source noise, it aids suppression of low-frequency BCS noise and improves temperature stability of the oscillator. It should be noted that a multi-layer inductor would also be suitable for L_{RID} as it requires even less chip area, as long as its self-resonant frequency is sufficiently greater than $2f_0$.

At 11.4 GHz, the resonant inductor parallel resistance (considering the 30 Ω series resistor as the dominant part of its series loss resistance) would be around 290 Ω, which is still a factor of almost 10 larger effective degeneration impedance of the inductor-resistor combination than that of a resistor only. This shows that mainly the resonant-inductive degeneration allows for a suppression of the bias current source noise (290 Ω from the RID at $2f_0$ versus 30 Ω series resistor at DC), while requiring a small voltage headroom (that across 30 Ω), thus not compromising the voltage swing of the oscillation signal across the *LC*-tank and phase noise. Moreover, the resistor in series with the degenerative inductor broadens the resonance whereby reducing the bias-current source high-frequency noise contribution to the phase noise across a range of frequencies. For example, for a low quality factor of the resonant *RLC* circuit of around three, a 3 dB bandwidth would be 1.8 GHz around 11.4 GHz, which translates to a range of 0.9 GHz around the resonant 5.7 GHz frequency where the bias current source noise would be suppresed. However, the resonant-inductive degeneration would be less effective for the frequencies far away from the resonance, in which case, a capacitor bank across base-emitter terminals of the bias current source transistors could be used to tune the resonant frequency.

Compromising between good phase noise, low power consumption, and large frequency tuning range (aiming at the upper 802.11a/HIPERLAN/802.16a band), the other oscillator circuit parameters have been determined. The 1.2 nH symmetric and differentially shielded *LC*-tank inductor (L in Fig. 10) has been designed using 4 um thick aluminum top metal. It has two turns, an outer dimension of 190 um, metal width of 10 um, and metal spacing of 5 um. Two n-type MOS varactors (C_v in Fig. 10) with 40 gates complete the *LC*-tank. Metal-insulator-metal capacitors C_A and C_B are 100 and 250 fF, respectively. Two common-collector output buffers interface the test oscillator and a 50 Ω measurement set-up, each consuming 1.1 mA of current. All the relevant phase-noise related circuit parameters are shown in Table I.

TABLE I
PHASE-NOISE RELATED PARAMETERS OF THE BIPOLAR LC-VCO SHOWN IN FIG. 10

parameter	value
G_{TK}	1/340S
n	1.6
k	10
L	1.2nH
$2L_{RID}$	2.6nH
C_B/C_A	250fF/100fF
f_0	5.7GHz

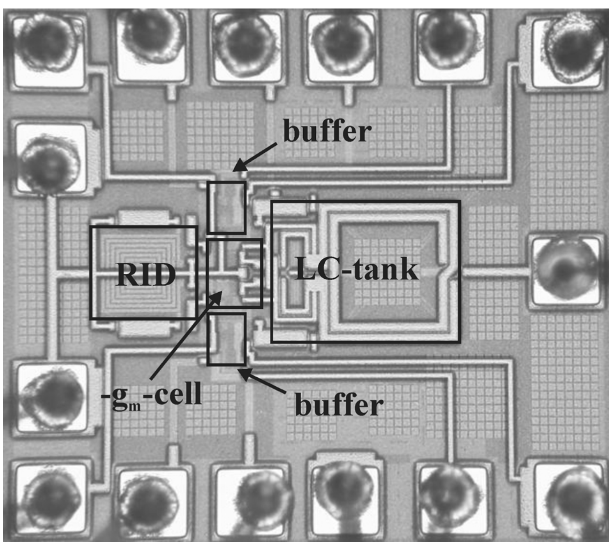

Fig. 11. Photomicrograph of the bipolar *LC*-VCO with resonant-inductive degeneration.

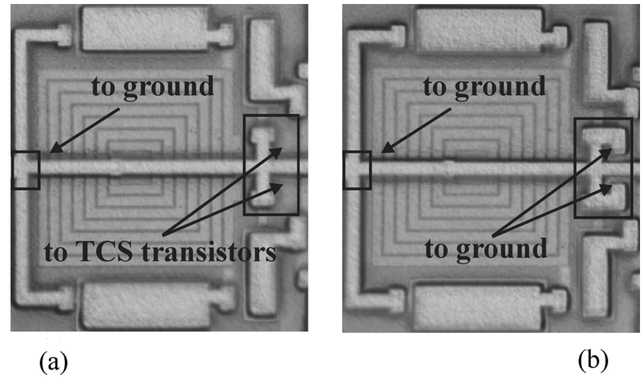

Fig. 12. (a) *LC*-VCO with resonant-inductive degeneration applied, (b) *LC*-VCO without RID applied.

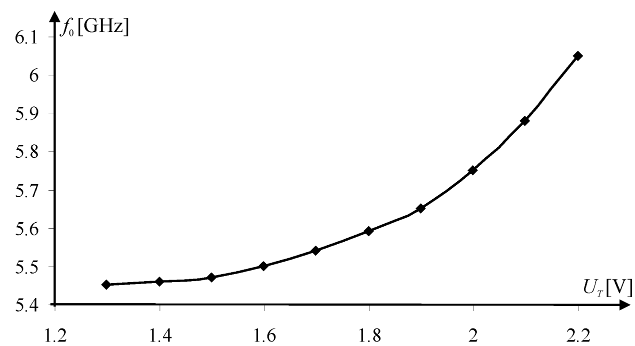

Fig. 13. Bipolar *LC*-VCO frequency tuning characteristic.

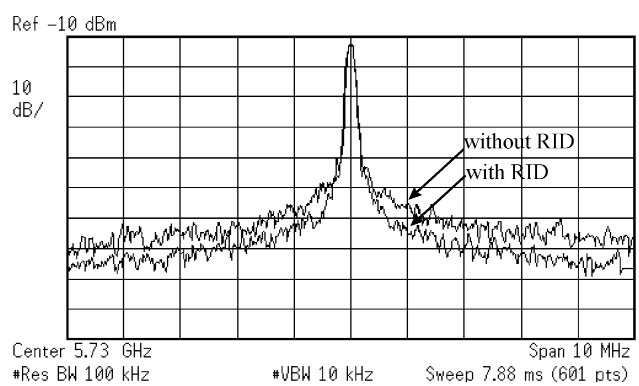

Fig. 14. Bipolar *LC*-oscillators output spectra in the 5.7 GHz band.

B. Experimental Results

The chip photomicrograph of the bipolar voltage-controlled oscillator with the RID is shown in Fig. 11, together with its buffer circuits. Inductors L_{RID} are grounded on one side only, as shown in Fig. 12(a), for the oscillator with the RID applied, and grounded on both sides, as shown in Fig. 12(b), for the oscillator without the RID applied. The two oscillator designs have maximum voltage swing and best phase noise for the same power consumption as they are identical, apart from the RID part.

The oscillator core occupies an area of 215×340 um^2, including buffers. After wirebonding into 32-lead quad packages, the oscillator design was connected to a printed-circuit board with bias and supply line filtering for testing [15].

A frequency tuning range of 600 MHz (5.45–6.05 GHz) was measured for a 0.9 V tuning voltage range (i.e., between 1.3 and 2.2 V of $V_{\rm TUNE}$) [1], [3], for both test oscillators, as shown in Fig. 13 (U_T stands for $V_{\rm TUNE}$). The error in the prediction of the oscillation frequency is below 1%. This frequency tuning range covers the upper band of 802.11a/HIPERLAN/802.16a standards, and with additional MOS capacitors in parallel with the LC-tank the operating frequency could be trimmed to cover the complete 5 GHz band.

Phase noise properties of the oscillators with and without resonant-inductive degeneration of the bias current source are compared in Fig. 14. For around -12 dBm output power from a single buffer (i.e., equal RF power levels of both oscillator outputs), the oscillator with the resonant-inductive degenerated bias current source has around 6 dB better phase noise at 1 MHz offset from the carrier in the 5.7 GHz band, compared to the oscillator implemented without resonant-inductive degeneration.

At 1 MHz offset from a 5.7 GHz carrier, the oscillator with the resonant-inductive degenerated bias current source achieves a phase noise of -112 dBc/Hz for a current consumption of 4.8 mA, as shown in Fig. 15.

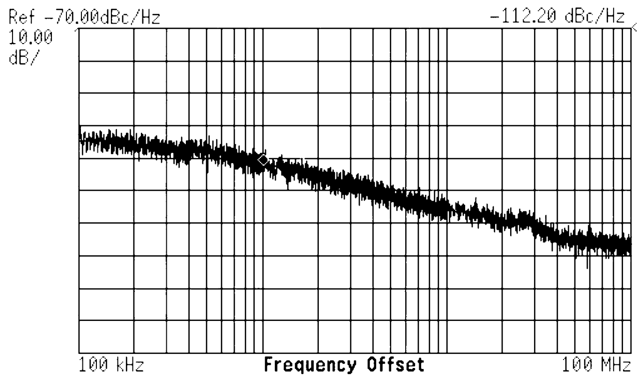

Fig. 15. Phase-noise plot of the test bipolar *LC*-oscillator in the 5.7 GHz band with resonant-inductive degeneration applied to the bias current source.

C. Discussion of Results for the LC-VCO With Resonant-Inductive Degeneration Applied

In this section, we compare the measurement results to the predictions of the oscillator phase-noise model [2], [3], for the bipolar *LC*-VCO with the resonant-inductive degeneration.

For a small-signal loop gain of $k \sim 10$, a capacitive divider ratio of $n \sim 1.6$, and a small start-up constant $c \sim 0.1$, the phase-noise performance of the oscillator biased from a common-emitter transistor is estimated from (9) as a factor 7.4 ($\sim$ 8.7 dB calculated, and $\sim$ 8.2 dB simulated) worse than that of an oscillator biased from a noiseless bias current source. From (6), the contribution of the undegenerated BCS noise to the phase noise of the oscillator is estimated at around 86%. If the noise from the bias current source were completely removed, we would expect a phase-noise improvement in the order of 8 dB from (34) and simulations.

However, the test oscillator circuit has recovered 6 dB of phase noise by means of the resonant-inductive degeneration of the bias current source. This difference may be explained as follows.

We have not opted for the highest $f_{T,CS}$ of the BCS transistor, thereby sacrificing the noise reduction. The reason for this choice is the expected higher current consumption than in the simulations, which would then shift the BCS transistor operation behind the point of a maximum $f_{T,CS}$. And indeed, the measurement results have shown that the quality of the LC-tank was overestimated in the simulations, and accordingly, the current consumption underestimated. As a result thereof, the resonant frequency between the L_{RID} and BCS base-emitter capacitor is different from $2f_0$, and the rejection of the BCS noise not complete.

Despite this, the 6 dB phase-noise improvement has been realized due to the robustness of the resonant-inductive degeneration technique. Better estimation of the oscillator operating point would allow for a complete phase-noise recovery with the method proposed.

VI. Conclusion

It has been shown that the contribution of the bias current source noise to the phase noise of the *LC* VCOs is larger than all other noise contributions put together. In particular, the bias current-source noise around twice the oscillation frequency degrades the phase noise most. Therefore, we have proposed resonant-inductive degeneration of the bias current source as a method to reduce this noise contribution. By forming a resonance between a degeneration inductor in the emitter lead of the bias current-source transistor and its base-emitter capacitance at twice the oscillation frequency, the contribution of the noise from the bias current source to the phase noise of bipolar oscillators is reduced by a square of the ratio of its transit frequency and twice the oscillation frequencies.

Two bipolar test oscillator circuits have been designed to verify the noise-reduction method proposed: one with and the other without resonant-inductive degeneration. Resonant-inductive degeneration in the emitter of the bias current-source transistor has improved the phase noise of a 5.7 GHz voltage-controlled oscillator by 6 dB.

Resonant-inductive degeneration is suitable for low-voltage RF applications, as it requires no DC voltage headroom. Moreover, a low-nH degenerative inductor required for GHz-range applications can be cost-effectively implemented in any modern multi-layer metal silicon technology.

References

[1] A. Tasić, W. A. Serdijn, J. R. Long, and D. Haramee, "Resonant-inductive degeneration for a fourfold phase-noise improvement of a 5.7 GHz band voltage-controlled oscillators," in *Proc. IEEE Bipolar/CMOS Circuit Technol. Meet.*, Oct. 2005, pp. 236–239.
[2] A. Tasić, W. A. Serdijn, and J. R. Long, *Adaptive Low-Power Circuits for Wireless Communications*. New York: Springer, 2006.
[3] A. Tasić, W. A. Serdijn, and J. R. Long, "Spectral analysis of phase noise in bipolar LC-oscillators—Theory, verification and design," *IEEE Trans. Circuits Syst. I, Reg. Papers*, to be published.
[4] *The IEEE 802.16 Working Group on Broadband Wireless Access Standards*, IEEE 802.16. [Online]. Available: http://www.ieee802.org/16/
[5] ETSI HIPERLAN/2 Standard [Online]. Available: http://portal.etsi.org/bran/kta/Hiperlan/hiperlan2.asp
[6] *Wireless LAN MAC and Physical Layer (PHY) Specification—High-Speed PHY in the 5 GHz Band*, ANS/IEEE Standard 802.11a, 1999.
[7] D. B. Leeson, "A simple model of feedback oscillator noise spectrum," *Proc. IEEE*, vol. 54, no. 2, pp. 329–330, Feb. 1966.
[8] S. P. Voinigescu, M. C. Maliepaard, J. L. Showell, G. E. Babcock, D. Marchesan, M. Schroter, P. Schvan, and D. L. Haram, "A scalable HF noise model for bipolar transistors with application to transistor sizing for LNA design," *IEEE J. Solid-State Circuits*, vol. 32, no. 9, pp. 1430–1439, Sep. 1997.
[9] A. van Staveren, C. Verhoeven, and A. van Roermund, *Structured Electronic Design: High-Performance Harmonic Oscillators and Bandgap References*. Boston, MA: Kluwer, 2001.
[10] J. Rael and A. Abidi, "Physical processes of phase noise in differential LC oscillators," in *Proc. CICC*, Sep. 2000, pp. 569–572.
[11] A. Hajimiri and T. Lee, "Design issues in CMOS differential LC oscillators," *IEEE J. Solid-State Circuits*, vol. 34, no. 5, pp. 717–724, May 1999.
[12] E. Hegazi, H. Sjoland, and A. A. Abidi, "Filtering technique to lower oscillator phase-noise," in *Proc. ISSCC*, Feb. 2001, pp. 364–365.
[13] P. Grey and R. Mayer, *Analysis and Design of Analog Integrated Circuits*, 2nd ed. New York: Wiley, 2001.
[14] P. Andreani and H. Sjoland, "Tail current noise suppression in RF CMOS VCOs," *IEEE J. Solid-State Circuits*, vol. 37, no. 3, pp. 342–348, Mar. 2002.
[15] A. Tasić, W. A. Serdijn, and J. R. Long, "Design of multi-standard adaptive voltage-controlled oscillators," *IEEE Trans. Microw.Theory Techn.*, vol. 53, no. 2, pp. 556–563, Feb. 2005.

Aleksandar Tasic received the M.Sc. degree in electronics and telecommunications from the Electronics Faculty, University of Nis, Nis, Serbia, in 1998, and the Ph.D. degree from the Faculty of Electrotechnics, Mathematics, and Informatics, the Delft University of Technology, Delft, the Netherlands, in 2005.

Between 1998 and 2000, he was a Research Assistant with the Electronics Faculty, University of Nis. Between 2005 and 2007, he was working as an Assistant Professor at the Electronics Research Laboratory/ DIMES, the Delft University of Technology. In 2005/2006, he was appointed as a Visiting Research Scientist at the University of California, San Diego. Since 2007, he has been with Qualcomm, San Diego, CA, first as a Senior and then as a Staff RF/Analog Engineer. His research interest includes design of adaptive and multistandard receiver circuits and systems for wireless communications.

Wouter A. Serdijn was born in Zoetermeer (“Sweet Lake City”), The Netherlands, in 1966. He received the “ingenieurs” (M.Sc.) degree from the Faculty of Electrical Engineering at the Delft University of Technology, Delft, The Netherlands, in 1989 and the Ph.D. degree from the Electronics Research Laboratory of the same university in 1994.

He teaches Analog Electronics for Electrical Engineers, Micropower Analog IC Techniques and Electronic Design Techniques. His research interests include low-voltage, ultra-low-power, high-frequency and dynamic-translinear analog integrated circuits along with circuits for RF and UWB wireless communications, hearing instruments and pacemakers. He authored and coauthored more than 150 publications and presentations.

Dr. Serdijn has served as an Associate Editor for the IEEE TRANSACTIONS ON CIRCUITS AND SYSTEMS—PART II: EXPRESS BRIEFS, as chair of the Analog Signal Processing Technical Chapter of the IEEE CAS society, and currently serves as an Associate Editor for the IEEE TRANSACTIONS ON CIRCUITS AND SYSTEMS—PART I: REGULAR PAPERS.

John R. Long received the B.Sc. in electrical engineering from the University of Calgary, Calgary, AB, Canada, in 1984, and the M.Eng. and Ph.D. degrees in electronics engineering from Carleton University, Ottawa, ON, Canada, in 1992 and 1996, respectively.

He was employed for 10 years by Bell-Northern Research, Ottawa involved in the design of ASICs for Gbit/s fiber-optic transmission systems and for 5 years at the University of Toronto. He joined the faculty at the Delft University of Technology, Delft, The Netherlands, in January 2002 as Chair of the Electronics Research Laboratory. His current research interests include: low-power transceiver circuitry for highly-integrated radio applications, and electronics design for high-speed data communications systems.